Int. J. Heat Mass Transfer. Vol. 29, No. 10, pp. 1521–1529, 1986
Printed in Great Britain

0017-9310/86 $3.00+0.00
Pergamon Journals Ltd.

The effects of temperature-dependent viscosity and coefficient of thermal expansion on the stability of laminar, natural convective flow along an isothermal, vertical surface

P. SABHAPATHY and K. C. CHENG†
Department of Mechanical Engineering, University of Alberta, Edmonton, Alberta, Canada

(*Received* 12 *December* 1985 *and in final form* 5 *May* 1986)

Abstract—The effects of temperature-dependent viscosity and coefficient of thermal expansion on the stability of laminar, natural convective boundary-layer flow of a liquid along an isothermal, vertical surface are studied employing linear stability theory for Prandtl numbers 7–10. Numerical solutions indicate that the temperature-dependent viscosity stabilizes the flow along a heated wall and destabilizes it along a cooled wall. The temperature-dependent coefficient of thermal expansion initially stabilizes the flow for a heated wall but farther downstream it destabilizes the flow. Flow visualization studies in water with an isothermal, vertical copper pipe (outside diameter 41.3 mm and length 1 m) for various combinations of wall and ambient temperatures in the range 5–35°C support the numerical predictions.

INTRODUCTION

IN THE theoretical analysis of the natural convective flow along an isothermal, vertical surface, it is customary to assume that the properties of the fluid are constant, except for density in the buoyancy force term of the momentum equation where it is assumed to vary linearly with temperature (Boussinesq approximations). This is true only if the temperature difference between the wall and the ambient medium is small. For example, for water at 15°C and 1 atm, Boussinesq approximations are strictly valid only when temperature difference is less than 1.25°C [1]. At larger temperature differences, the effects of variable properties should be included in the analysis. This is especially true of viscosity and coefficient of thermal expansion in the case of liquids [2–4]. The effects of variable properties on the laminar, natural convective flow along an isothermal, vertical surface have been extensively studied in the past and a literature review can be found in ref. [4].

Near the leading edge of the vertical surface the natural convective flow is always laminar. Away from the leading edge, the laminar flow becomes unstable due to ever-present disturbances in the system. The thermal transport is different in laminar, transition and turbulent flow regimes. Hence the knowledge of the nature of the flow is important for estimating the thermal transport. The transition from laminar to turbulent regime depends on the stability characteristics of the flow. Stability and transition to turbulence of the natural convective flow along a vertical surface have been extensively studied by many investigators employing Boussinesq approximations. Literature reviews can be found in refs. [4, 5].

† To whom correspondence should be addressed.

In the forced convective flow of a liquid over a flat plate, the variation of viscosity with temperature destabilizes the flow for a cooled wall, and stabilizes the flow for a heated wall [6, 7]. For the natural convective boundary-layer flow along an isothermally heated, vertical flat plate, Piau [2] has shown that the variation of viscosity may have a stabilizing effect for a heated wall. Recently, Higgins and Gebhart [8, 9] studied the stability of buoyancy-induced flows in cold water along an isothermal, vertical flat plate. They found that the Boussinesq approximation over-predicts the buoyancy force for up flows with the resulting neutral stability curves lying to the left of the true ones. The opposite remarks are true for down flows.

In this paper, the effects of variations of viscosity and coefficient of thermal expansion with temperature on the stability of laminar, natural convective boundary-layer flow of a liquid along an isothermal, vertical flat plate are studied numerically employing linear stability theory for Prandtl numbers 7–10. Both cooled and heated walls are examined. The results for the onset of instability and the transition to turbulent flow obtained from flow visualization studies in water with an isothermal, vertical, circular cylinder for various combinations of wall and ambient water temperatures in the range 5–35°C are also presented.

THEORETICAL ANALYSIS

Governing equations

The coordinate system is shown in Fig. 1. The quiescent ambient liquid and the surface of the vertical flat plate are at constant temperatures t_∞ and t_0, respectively. The dynamic viscosity μ and density ρ are assumed to be functions of temperature alone. The

NOMENCLATURE

A	disturbance amplification factor, equation (24)
A_c, A_G	disturbance amplitudes, equation (24)
B_1, B_2, B_3	complex constants, equations (19) and (20)
c	dimensionless wave velocity, β/α
c_p	specific heat at constant pressure
C_1, C_2, C_3	real constants, equations (17) and (18)
F	similarity streamfunction
g	acceleration due to gravity
G	$4[Gr_x/4]^{1/4}$
Gr_x	Grashof number, $g(\rho_0-\rho_\infty)x^3/(\rho_0\nu_f^2)$
i	$\sqrt{-1}$
k	thermal conductivity
Pr	Prandtl number, $\mu_f c_p/k$
q	constant, equation (17)
Ra_x	Rayleigh number, $Gr_x Pr$
s	temperature disturbance amplitude function
t	temperature
u, v	velocity components in x and y directions
x, y	Cartesian coordinates.

Greek symbols

α	complex wave number
β	coefficient of thermal expansion, main flow equations
β	real frequency, disturbance equations
γ	parameter for the variation of viscosity with temperature, equation (7)
δ	boundary-layer thickness
ε	parameter for the variation of coefficient of thermal expansion with temperature, equation (10)
η	similarity variable
θ	dimensionless temperature, $(\bar{t}-t_\infty)/(t_0-t_\infty)$
λ	constant, equation (17)
μ	dynamic viscosity
ν	kinematic viscosity
ρ	density
ϕ	velocity disturbance amplitude function
ψ	streamfunction.

Subscripts

f	'film' condition
0	at the wall
∞	ambient condition.

Superscripts

$\bar{}$	mean value
$\tilde{}$	dimensional quantity
$'$	differentiation with respect to η.

thermal conductivity k and specific heat c_p are assumed to be constant. For moderate temperature differences ($\sim$ 10–50°C in the case of water at 1 atm, for example) between the wall and the ambient liquid, the density can be assumed to be constant in terms other than the buoyancy force term of the governing equations [4]. The dissipation terms due to pressure and viscosity can be also neglected.

The base flow equations are the boundary-layer equations. Employing the similarity variables technique, the resulting base flow equations become [4]

$$\frac{\mathrm{d}}{\mathrm{d}\eta}\left[\frac{\mu}{\mu_f}F''\right]+3FF''-2(F')^2+\frac{\rho_\infty-\bar{\rho}}{\rho_\infty-\rho_0}\frac{\rho_0}{\bar{\rho}}=0 \quad (1)$$

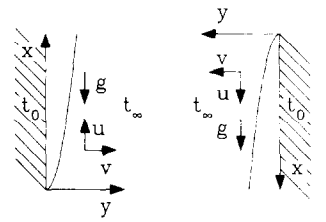

(a) Up Flow (b) Down Flow

FIG. 1. Coordinate system.

$$\theta''+3Pr F\theta'=0 \quad (2)$$

$$F(0)=F'(0)=\theta(0)-1=F'(\infty)=\theta(\infty)=0 \quad (3)$$

where

$$Gr_x=\frac{g(\rho_\infty-\rho_0)x^3}{\rho_0\nu_f^2},\quad G=4\left[\frac{Gr_x}{4}\right]^{1/4},\quad \eta=\frac{Gy}{4x} \quad (4)$$

$$\bar{\psi}=\nu_f G F(\eta),\quad \theta=\frac{\bar{t}-t_\infty}{t_0-t_\infty} \quad (5)$$

$$\bar{u}=\frac{\partial\bar{\psi}}{\partial y},\quad \bar{v}=-\frac{\partial\bar{\psi}}{\partial x}. \quad (6)$$

For moderate temperature differences between the surface and the ambient liquid, the ratio μ/μ_f can be approximated by a linearized Taylor series expansion about a reference temperature. Taking the reference temperature to be the film temperature, the linearized approximation can be written as [1, 3, 4]

$$\frac{\mu}{\mu_f}=1+\frac{1}{\mu_f}\left.\frac{\mathrm{d}\mu}{\mathrm{d}\bar{t}}\right|_f(\bar{t}-t_f)=1+\gamma_f(\theta-\tfrac{1}{2}) \quad (7)$$

where

$$\gamma_f=\frac{1}{\mu_f}\left.\frac{\mathrm{d}\mu}{\mathrm{d}\bar{t}}\right|_f(t_0-t_\infty). \quad (8)$$

For linear variation of viscosity with temperature

$$\gamma_f = 2\frac{(\mu_0/\mu_\infty - 1)}{(\mu_0/\mu_\infty + 1)}. \tag{9}$$

For moderate temperature differences between the surface and the ambient liquid, $\rho_0/\bar{\rho} \cong 1$. When the density is assumed to vary parabolically with temperature, the dimensionless buoyancy force term becomes [4]

$$\frac{\rho_\infty - \bar{\rho}}{\rho_\infty - \rho_0}\frac{\rho_0}{\bar{\rho}} \cong \theta[1-\varepsilon_f(1-\theta)] \tag{10}$$

where

$$\varepsilon_f = \frac{\beta_0 - \beta_\infty}{\beta_0 + \beta_\infty}. \tag{11}$$

The viscosity of a liquid decreases with an increase in temperature. Hence, for the linear variation of viscosity with temperature, γ_f varies from $+2$ to -2, positive for a cooled wall and negative for a heated one. For most liquids, and for water when the temperatures are higher than 4°C, ε_f varies from $+1$ to -1, positive for up flows (heated walls) and negative for down flows (cooled walls). Boussinesq approximations correspond to $\gamma_f = \varepsilon_f = 0$.

The disturbance equations are obtained by employing the assumptions involved in linear stability theory, such as small disturbances, parallel flow approximation, and are given in detail in ref. [4]. Assuming the disturbances to be two-dimensional travelling waves and non-dimensionalizing the variables, one obtains

$$[\phi'''' - 2\alpha^2\phi'' + \alpha^4\phi][1+\gamma_f(\theta-\tfrac{1}{2})]$$
$$= i\alpha G[(F'-c)(\phi''-\alpha^2\phi) - F''''\phi] - 2\gamma_f\theta'(\phi''' - \alpha^2\phi')$$
$$-\gamma_f\theta''(\phi''+\alpha^2\phi) - 2\varepsilon_f\theta' s - [1+2\varepsilon_f(\theta-\tfrac{1}{2})]s' \tag{12}$$

$$s'' - \alpha^2 s = i\alpha GPr[(F'-c)s - \phi'\theta'] \tag{13}$$

$$\phi(0) = \phi'(0) = s(0) = \phi(\infty) = \phi'(\infty) = s(\infty) = 0 \tag{14}$$

where

$$\delta = \frac{4x}{G}, \quad \alpha = \hat{\alpha}\delta, \quad \beta = \frac{4\hat{\beta}\delta x}{\nu_f G^2}, \quad c = \frac{\beta}{\alpha} \tag{15}$$

$$\phi(\eta) = \frac{4\hat{\phi}x}{\delta\nu_f G^2}, \quad s(\eta) = \frac{\hat{s}}{(t_0 - t_\infty)}. \tag{16}$$

Numerical method

The numerical method employed to solve the main flow and the disturbance equations was the same as the one given by Hieber and Gebhart [10]. At large η, the solutions to the base flow equations (1)–(3) are given by

$$F = C_1 + C_3 e^{-3C_1\eta/\lambda} + \frac{C_2 q}{[27C_1^3Pr^2(\lambda Pr - 1)]} e^{-3C_1Pr\eta} \tag{17}$$

$$\theta = C_2 e^{-3C_1Pr\eta} \tag{18}$$

where $\lambda = 1-(\gamma_f/2)$, $q = 1-\varepsilon_f$, and C_1, C_2 and C_3 are real constants.

The equations (1)–(3) were integrated numerically across the boundary layer from the outer edge to the wall, assuming some values for C_1, C_2 and C_3. The boundary conditions were checked at $\eta = 0$. The shooting method was employed to correct the values of C_1, C_2 and C_3 so that the boundary conditions were satisfied at $\eta = 0$. The solution was assumed to have converged when the relative errors in C_1, C_2 and C_3, and the absolute errors in the boundary conditions at $\eta = 0$ were less than 1×10^{-6}.

The system of equations (12)–(14) is a sixth-order eigenvalue problem, linear in the disturbance amplitudes ϕ and s. The solutions to the equations (12)–(14) can be written as a linear combination of six independent integrals as [10]

$$\phi(\eta) = B_1\phi_1 + B_2\phi_2 + B_3\phi_3 \tag{19}$$

$$s(\eta) = B_1 s_1 + B_2 s_2 + B_3 s_3 \tag{20}$$

where B_1, B_2 and B_3 are complex constants. B_1 was taken as 1.0, thus fixing the disturbance level arbitrarily. The integrals can be obtained from the solution of disturbance equations (12)–(14) at large values of η. They are given by

$$\phi_1 = e^{-\alpha\eta}, \quad \phi_2 = e^{-\alpha_2\eta} \tag{21}$$

$$\phi_3 = \frac{q(\alpha_3/\lambda)e^{-\alpha_3\eta}}{[(\alpha_3^2-\alpha^2)(\alpha_3^2-\alpha_2^2)]}, \quad s_1 = \frac{i\alpha PrG\theta'_\infty e^{-\alpha\eta}}{[\alpha_3^2-(3C_1Pr+\alpha)^2]} \tag{22}$$

$$s_2 = \frac{i\alpha PrG\theta'_\infty e^{-\alpha_2\eta}}{[\alpha_3^2-(3C_1Pr+\alpha_2)^2]}, \quad s_3 = e^{-\alpha_3\eta} \tag{23}$$

where

$$\alpha_2 = +\left[\alpha^2 - \frac{i\alpha cG}{\lambda}\right]^{1/2}, \quad \alpha_3 = +[\alpha^2 - i\alpha cPrG]^{1/2}.$$

For given values of G and β, a complex value for α was assumed. Starting with equations (19) and (20) as the initial values, the equations (12)–(14) were integrated across the boundary layer using a fourth-order Runge–Kutta method. B_2 and B_3 were determined by satisfying two of the three boundary conditions at $\eta = 0$. The remaining boundary condition at $\eta = 0$ is satisfied only if the assumed value of α is the eigenvalue of the equations (12)–(14). The value of α which satisfied the third boundary condition at $\eta = 0$ within a value of 1×10^{-6} was found iteratively.

RESULTS AND DISCUSSION

Equations (1)–(3) and (12)–(14) were solved numerically and the stability plane was obtained for various values of Pr, γ_f and ε_f. The numerical solutions agreed very well with those given by Nachtsheim [11] for $Pr = 0.733$, and $Pr = 6.7$ when $\gamma_f = \varepsilon_f = 0$. The details can be found in ref. [4].

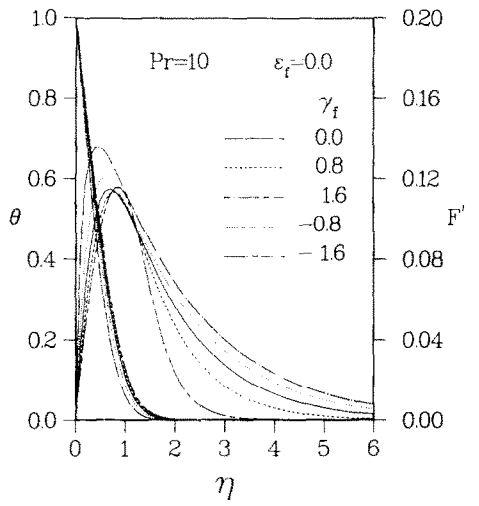

FIG. 2. The effects of γ_f on the base flow temperature and velocity profiles for $Pr = 10$.

The effects of variation of viscosity with temperature

The effects of temperature-dependent viscosity on the base flow temperature and velocity profiles for $Pr = 10$ are shown in Fig. 2 in terms of the parameter γ_f. As indicated earlier, for liquids, a positive value of γ_f denotes a cooled wall and a negative value, a heated wall. For a positive value of γ_f, the liquid near the wall is more viscous than that away from the wall. Numerical solutions, similar to the ones given in ref. [3], show that for a positive value of γ_f, the velocity boundary layer is smaller and the temperature boundary layer is slightly larger. The position of maximum velocity is farther from the wall and the total mass flow rate is lower. The larger the positive value of γ_f, the more pronounced are the effects. The opposite trends are true for a negative value of γ_f.

The effects of temperature-dependent viscosity on the stability of the laminar boundary-layer flow of a liquid with $Pr = 10$ are shown in Figs. 3–5. The stability plane shown in Fig. 3 corresponds to that of Boussinesq approximations ($\gamma_f = \varepsilon_f = 0$). The stability plane for a cooled wall (γ_f is positive) is shown in Fig. 4

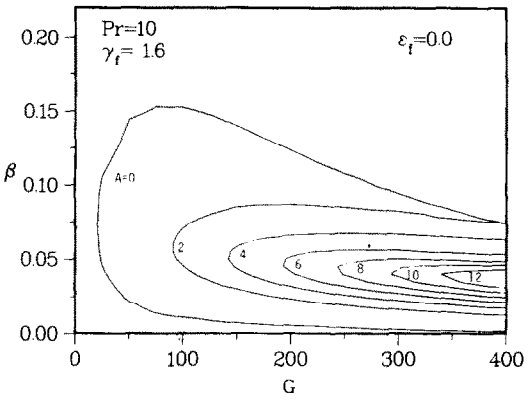

FIG. 4. The stability plane for $Pr = 10$ and $\gamma_f = 1.6$.

and that for a heated wall (γ_f is negative) is shown in Fig. 5. The stability of laminar flow depends on the amplification or decay of disturbance present in the system. If the disturbances amplify, as they move downstream, the flow is said to be unstable; if they decay, the flow is said to be stable. The rate of amplification (or decay) of a disturbance depends on the variation of α_i with G. At the neutral line, the rate of amplification is zero. If A_c is the amplitude of a disturbance on the neutral curve ($G = G_c$), its amplitude A_G at a location G is given by [10]

$$\frac{A_G}{A_c} = \exp(A) \tag{24}$$

where

$$A = -\frac{1}{3}\int_{G_c}^{G} \alpha_i \, dG.$$

Contours of A were obtained by following various constant frequency paths and evaluating the above integral along these paths. By comparing the neutral stability curves ($A = 0$) in Figs. 3–5, it can be clearly seen that the laminar flow becomes unstable at a lower value of G for a cooled wall than for a heated wall.

The transition from laminar into turbulent flow depends on the growth of the disturbances as they move downstream. It is seen that the amplification of

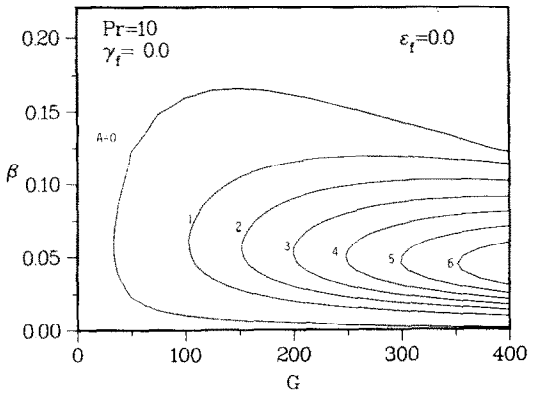

FIG. 3. The stability plane for $Pr = 10$ and $\gamma_f = 0.0$.

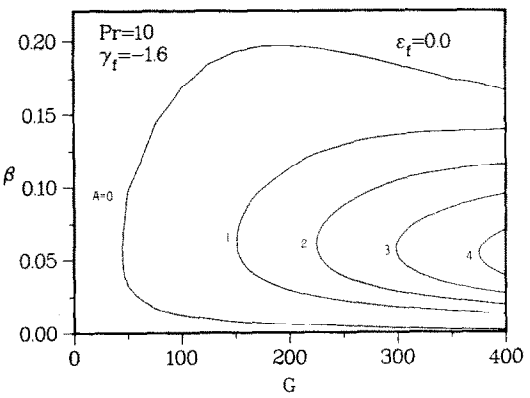

FIG. 5. The stability plane for $Pr = 10$ and $\gamma_f = -1.6$.

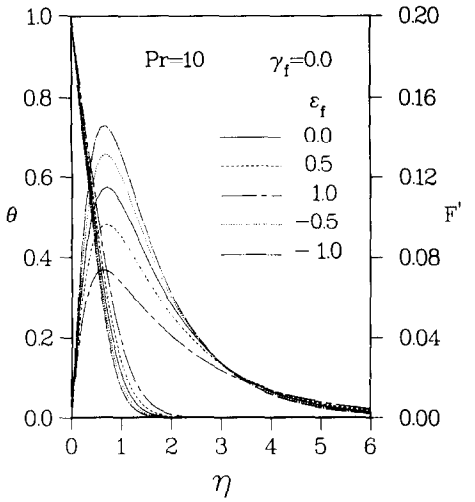

FIG. 6. The effects of ε_f on the base flow temperature and velocity profiles for $Pr = 10$.

disturbances is faster for a positive value of γ_f than for a negative value (compare the contours of $A = 4$, for example). The frequency filtering mechanism is also more pronounced for a positive value. The larger the positive value, the more pronounced are the effects. Hence, as in forced convection, for liquids, the flow is more unstable for a cooled wall than for a heated wall with the same film temperature. As the disturbances amplify faster for a cooled wall, the transition to turbulent flow may occur earlier.

The effects of variation of coefficient of thermal expansion with temperature

The effects of temperature-dependent coefficient of thermal expansion on the base flow temperature and velocity profiles for $Pr = 10$ are shown in Fig. 6 in terms of the parameter ε_f. As indicated earlier, for most liquids, and for water when the temperatures are higher than 4°C, a negative value of ε_f denotes a cooled wall (down flow) and a positive value denotes a heated wall (up flow). The dimensionless buoyancy force at any point inside the thermal boundary layer is larger for a negative value of ε_f than for a positive value [see equation (10)]. Numerical solutions indicate that for a negative value of ε_f, the total mass flow rate and the value of maximum velocity are higher, and the thermal boundary-layer thickness is smaller. The larger the absolute value of ε_f, the more pronounced are the effects.

Figures 7 and 8 show the stability planes for $\varepsilon_f = 1.0$ and -1.0, respectively for $Pr = 10$. From Figs. 3, 7 and 8, it can be seen that the neutral stability curve for a negative value of ε_f lies left of the one for a positive value. Hence, the critical Grashof number for the onset of instability is lower for down flows than that for up flows. These trends agree with those of Higgins and Gebhart [8, 9]. But, the amplification of disturbances, as they move downstream, is faster for a positive value of ε_f than for a negative value (compare

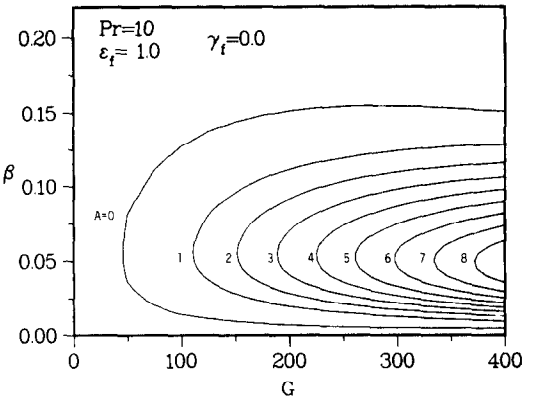

FIG. 7. The stability plane for $Pr = 10$ and $\varepsilon_f = 1.0$.

the contours of $A = 6$, for example). Hence, for most liquids, the temperature-dependent coefficient of thermal expansion initially stabilizes the flow for a heated wall but farther downstream it destabilizes the flow.

The effects of both the variation of viscosity and the coefficient of thermal expansion with temperature

For many liquids, in particular for water and aqueous solutions, both the viscosity and the coefficient of thermal expansion are strong functions of temperature. Hence it is important to consider the effects of both γ_f and ε_f on the stability of laminar, natural convective flow along an isothermal, vertical flat plate.

Numerical solutions were obtained for typical cases of natural convective flow from an isothermal, vertical flat plate in water for $t_f = 10$°C with $|t_0 - t_\infty| = 10$°C, and for $t_f = 20$°C with $|t_0 - t_\infty| = 20$°C. The Prandtl numbers for these cases are 9.34 and 7.0, respectively. For the cooled wall, the approximate values of γ_f and ε_f are 0.29, −0.81 and 0.50, −0.55, respectively. For the heated wall, the values are −0.29, 0.81 and −0.50, 0.55, respectively. The case of $\gamma_f = \varepsilon_f = 0$ corresponds to Boussinesq approximations. The base flow temperature and velocity profiles are shown in Fig. 9 for $Pr = 7.0$. It can be seen that the effects of γ_f and ε_f

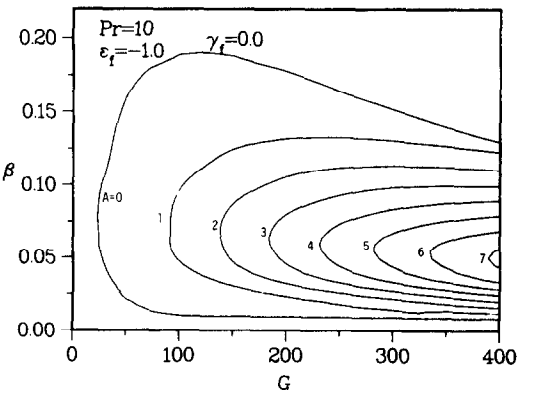

FIG. 8. The stability plane for $Pr = 10$ and $\varepsilon_f = -1.0$.

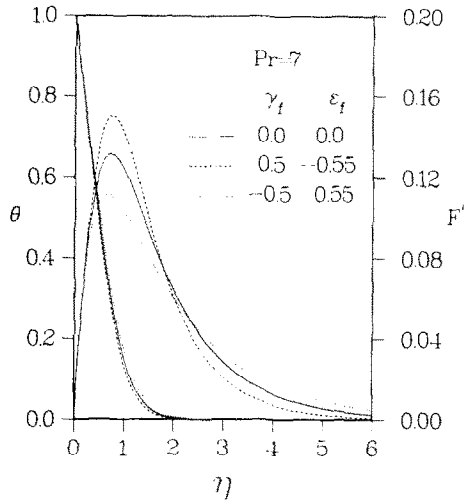

FIG. 9. Base flow temperature and velocity profiles for water, when $t_f = 20°C$ and $|t_0 - t_\infty| = 20°C$.

normally oppose each other. For the cooled wall, the maximum velocity is larger and the boundary-layer thickness is smaller. For the heated wall, the maximum velocity is lower and the boundary-layer thickness is larger. The mass flow rate was found to be slightly larger for the cooled wall.

The effects of both γ_f and ε_f on the stability of the laminar flow are shown in Figs. 10 and 11. For the cooled wall, the critical Grashof number for the onset of instability is lower and the rate of amplification of disturbance is faster for the variable property case than for the Boussinesq approximations. For the heated wall, the effect of variable properties is to stabilize the flow initially (compare the neutral stability curves in Figs. 10 and 11), but the disturbances amplify faster at downstream locations (compare the contours of $A = 6$ in Fig. 10, for example). Although in Fig. 11, the contour of $A = 4$ for the heated wall is to the left of that for the Boussinesq approximations; farther downstream, the disturbance may amplify faster for the case of variable property (as was the case in Fig. 10). The larger the absolute values of γ_f and ε_f, the more pronounced are

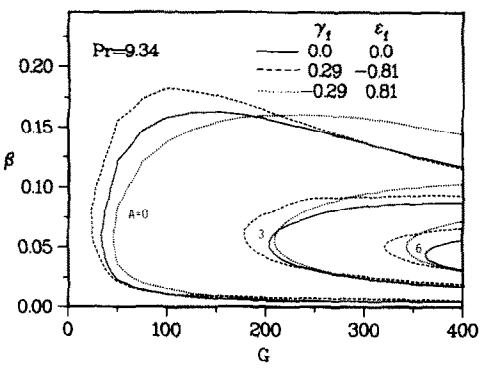

FIG. 10. The effects of both γ_f and ε_f on the stability of laminar flow of water, when $t_f = 10°C$ and $|t_0 - t_\infty| = 10°C$.

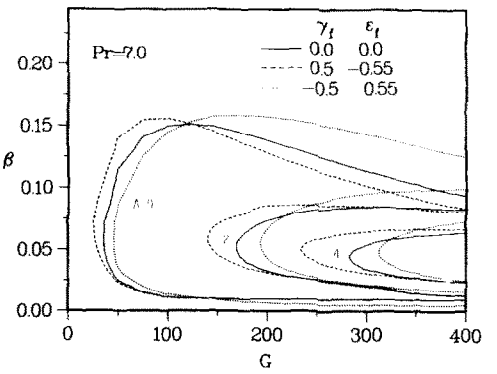

FIG. 11. The effects of both γ_f and ε_f on the stability of laminar flow of water, when $t_f = 20°C$ and $|t_0 - t_\infty| = 20°C$.

their effects on the stability of the laminar flow. Hence, the laminar, natural convective flow of a liquid along an isothermal, vertical wall is more unstable for larger temperature differences between the wall and the ambient medium.

Flow visualization studies

Flow visualization experiments were conducted in water with an isothermal, vertical, circular cylinder for various combinations of wall and ambient temperatures in the range 5–35°C. The purpose of these experiments was to study qualitatively the effects of variable properties on the onset of instability and the transition to turbulence of the natural convective flow in water. The experimental apparatus shown in Fig. 12 is described in detail in ref. [4]. The test section, a 1-m-long copper pipe with an outside diameter of 41.3 mm and a wall thickness of 3 mm, was in the center of a large insulated water tank (0.6 m long, 0.6 m wide and 1.6 m high). The test section was cooled or heated to the desired temperature by circulating water at a high flow rate ($\sim 1 \times 10^{-2}\,m^3\,s^{-1}$) from a constant temperature bath. The surface temperature of the copper pipe was taken as the average of the inlet and the outlet water temperatures. The water tank had plexiglass windows for flow visualization. Flow visualization techniques used were the shadowgraph and the dye injection methods.

The tank was filled with deaerated plain tap water and was allowed to equilibrate for about 1–2 h. The cooling or heating water from the constant temperature bath was then circulated through the test section. About 15 min after starting the experiment, the locations of the onset of instability and the transition to turbulent flow were closely observed for the naturally occurring disturbances. The onset of instability was taken as the nearest point from the leading edge where small oscillations on the dye were observed. The disturbances, as they moved downstream, amplified with time and distance, and became vortices. Soon the vortices broke down into turbulent flow. The point of transition to turbulent

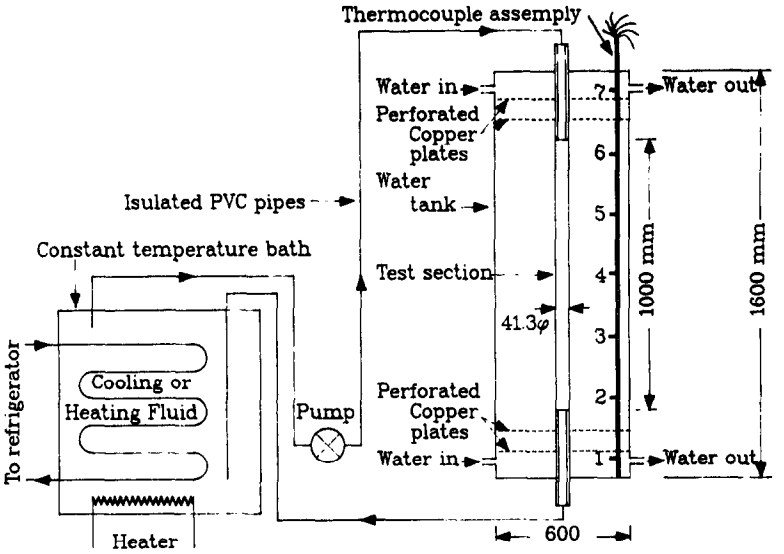

FIG. 12. Schematic diagram of the experimental apparatus.

flow was taken as the nearest point from the leading edge below which the flow was always turbulent. The turbulent flow exhibited the nature of complete disorder and mixing. The experiment was repeated for various combinations of wall and ambient temperatures in the range 5–35°C.

Figure 13 shows a typical shadowgraph when $t_0 = 5.0$°C and $t_\infty = 28.0$. For this case, the onset of instability and the transition to turbulent flow were approximately 16.0 and 57.5 cm respectively from the leading edge. Figure 14 shows the critical values of Rayleigh number for the onset of instability and the transition to turbulent flow for various temperature differences between the wall and the ambient water. The results for a vertical, circular cylinder can be assumed to be that of a flat plate if $(d/x)(Ra_x)^{1/4} > M$ where d is the diameter, x is the distance from the leading edge to the point of measurement and M is a constant. The validity of this assumption has been discussed by Fujii *et al.* [12]. It is to be noted that the value of M for the experiments conducted in the present study was within that of ref. [12]. The critical values of Ra_x for the transition to turbulent flow also agreed well with those of ref. [12]. The critical values of Ra_x for the transition to turbulent flow were found to be independent of the Prandtl number for temperature range investigated.

The experimentally obtained critical values Ra_x for the onset of instability are 3–4 orders of magnitude higher than those obtained numerically. This is due to the fact that the naturally occurring disturbance could be detected experimentally only when its amplitude was finite whereas the analysis based on linear stability theory assumed an infinitesimal value. For larger temperature differences between the wall and the ambient medium, the critical values of Ra_x for the onset of instability and transition to turbulent flow obtained experimentally are lower for both cooled and heated walls. It is to be noted that the linear stability analysis predicted these trends to be true at locations farther away from the point of onset of instability (see Fig. 10, for example).

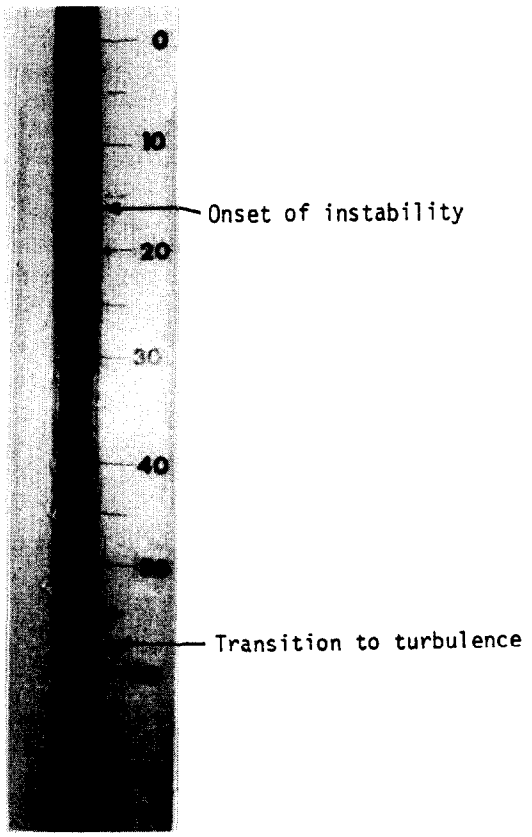

FIG. 13. Photograph of shadowgraph flow visualization in water for $t_0 = 5.0$°C and $t_\infty = 28.0$°C.

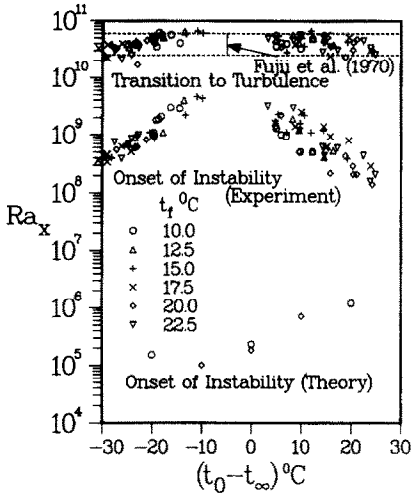

FIG. 14. The experimentally obtained critical values of Ra_x in water.

CONCLUSIONS

The effects of the variations of viscosity and coefficient of thermal expansion with temperature were examined for the laminar, natural convective boundary-layer flow of a liquid along an isothermal, vertical flat plate. Numerical results show that the temperature-dependent viscosity stabilizes the flow for a heated wall and destabilizes it for a cooled wall. The frequency filtering mechanism is more pronounced for a cooled wall. The variation of coefficient of thermal expansion with temperature lowers the critical Grashof number for the onset of instability for a cooled wall but the disturbance growth rate is faster for a heated wall. Hence, the temperature-dependent coefficient of thermal expansion initially stabilizes the flow for a heated wall, but farther downstream it destabilizes the flow. The trends of experimentally obtained critical values of Grashof number for the onset of instability and the transition to turbulent flow support the numerical predictions.

Acknowledgement—This work was supported by an operating grant from the Natural Sciences and Engineering Research Council of Canada.

REFERENCES

1. D. D. Gray and A. Giorgini, The validity of Boussinesq approximations for liquids and gases, *Int. J. Heat Mass Transfer* **19**, 545–551 (1976).
2. J.-M. Piau, Influence des variations des propriétés physiques et de la stratification en convection naturelle, *Int. J. Heat Mass Transfer* **17**, 465–476 (1974).
3. V. P. Carey and J. C. Mollendorf, Natural convection in liquids with temperature dependent viscosity, *Proc. 6th Int. Heat Trans. Conf.* **NC-5**, pp. 211–216 (1978).
4. P. Sabhapathy, Natural convection in liquids with temperature-dependent properties and solidification. Ph.D. thesis, University of Alberta, Edmonton, Canada (1986).
5. B. Gebhart and R. L. Mahajan, Instability and transition in buoyancy induced flows, *Adv. appl. Mech.* **22**, 231–315 (1982).
6. E. G. Hauptmann, The influence of temperature dependent viscosity on laminar boundary-layer stability, *Int. J. Heat Mass Transfer* **11**, 1049–1052 (1968).
7. A. R. Wazzen, T. Okamura and A. M. O. Smith, The stability of water flow over heated and cooled flat plates, *Trans. Am. Soc. mech. Engrs*, Series C, *J. Heat Transfer* **68**, 109–113 (1968).
8. J. M. Higgins and B. Gebhart, Measurements of instability and disturbance growth in vertical buoyancy induced flows in cold water, *Int. J. Heat Mass Transfer* **25**, 1397–1409 (1982).
9. J. M. Higgins and B. Gebhart, Stability of vertical buoyancy induced flows in cold water, *Trans. Am. Soc. mech. Engrs*, Series C, *J. Heat Transfer* **105**, 767–773 (1983).
10. C. A. Hieber and B. Gebhart, Stability of vertical natural convection boundary layers: some numerical solutions, *J. Fluid Mech.* **48**, 625–648 (1971).
11. P. R. Nachtsheim, Stability of free-convection boundary layer flows, NASA TN D-2089 (1963).
12. T. Fujii, M. Takeuchi, M. Fujii, K. Suzaki and H. Uehara, Experiments on natural convective heat transfer from the outer surface of a vertical cylinder to liquids, *Int. J. Heat Mass Transfer* **13**, 753–787 (1970).

LES EFFETS DE LA VISCOSITE ET DU COEFFICIENT DE DILATATION THERMIQUE VARIABLES SUR LA STABILITE DE LA CONVECTION NATURELLE LAMINAIRE LE LONG D'UNE SURFACE ISOTHERME ET VERTICALE

Résumé—Les effets de la viscosité et du coefficient de dilatation thermique dépendant tous deux de la température sur la stabilité de l'écoulement de couche limite en convection naturelle, laminaire, d'un liquide le long d'une surface isotherme et verticale sont étudiés en utilisant la théorie de la stabilité linéaire pour des nombres de Prandtl de 7 à 10. Des solutions numériques montrent que la viscosité variable avec la température stabilise l'écoulement le long d'une paroi chaude et le déstabilise le long d'une paroi froide. Le coefficient de dilatation variable avec la température stabilise initialement l'écoulement pour un mur chaud, mais en aval il le déstabilise. Des visualisations dans l'eau avec tuyau de cuivre isotherme et vertical (diamètre extérieur 41,3 mm et longueur 1 m) pour différentes combinaisons de températures de paroi et ambiantes dans le domaine 5–35°C confirment les prédictions numériques.

STABILITÄT EINER LAMINAREN NATÜRLICHEN KONVEKTIONSSTRÖMUNG

Zusammenfassung—Der Einfluß der Temperaturabhängigkeit von Zähigkeit und Volumenausdehnungskoeffizient auf die Stabilität einer laminaren natürlichen Grenzschichtströmung einer Flüssigkeit

entlang einer isothermen vertikalen Oberfläche wird mit Hilfe der linearen Stabilitätstheorie für Prandtl-Zahlen zwischen 7 und 10 untersucht. Numerische Lösungen zeigen, daß die temperaturabhängige Zähigkeit zu einer Stabilisierung entlang einer beheizten Wand führt, während sie entlang einer gekühlten Wand destabilisierend wirkt. Der temperaturabhängige Volumenausdehnungskoeffizient führt anfangs zu einer Stabilisierung der Strömung an der beheizten Wand, bei größerer Lauflänge jedoch wirkt er destabilisierend. Eine visuelle Untersuchung der Strömung von Wasser an einem isothermen vertikalen Kupferrohr (Außendurchmesser 41,3 mm, Länge 1 m) bei verschiedenen Wand- und Wassertemperaturen im Bereich von 5 bis 35°C bestätigen die numerischen Berechnungen.

ВЛИЯНИЕ ТЕМПЕРАТУРНЫХ ЗАВИСИМОСТЕЙ ВЯЗКОСТИ И КОЭФФИЦИЕНТА ТЕПЛОВОГО РАСШИРЕНИЯ НА УСТОЙЧИВОСТЬ ЛАМИНАРНОГО ТЕЧЕНИЯ ПРИ ЕСТЕСТВЕННОЙ КОНВЕКЦИИ У ИЗОТЕРМИЧЕСКОЙ ВЕРТИКАЛЬНОЙ ПОВЕРХНОСТИ

Аннотация—На основе линейной теории устойчивости при числах Прандтля от 7 до 10 исследовано влияние температурных зависимостей вязкости и коэффициента теплового расширения на устойчивость ламинарного течения жидкости в пограничном слое при естественной конвекции у изотермической вертикальной поверхности. Из численных решений следует, что учет температурной зависимости вязкости приводит к стабилизации течения у нагретой поверхности и к дестабилизации у охлажденной. Учет температурной зависимости коэффициента теплового расширения для нагретой стены на начальном участке стабилизирует течение, но затем (ниже по потоку) дестабилизирует его. Визуализация течения в изотермической вертикальной медной трубе длиной 1 м и с наружным диаметром 41,3 мм при различных сочетаниях температуры стенки и окружающей среды в диапазоне 5–35°C подтверждает численные расчеты.